

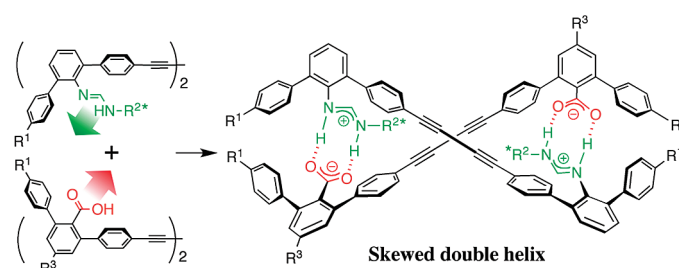
Double-Stranded Supramolecular Assembly through Salt Bridge Formation between Rigid and Flexible Amidine and Carboxylic Acid Strands

Hiroki Iida, Munenori Shimoyama, Yoshio Furusho, and Eiji Yashima*

Department of Molecular Design and Engineering, Graduate School of Engineering, Nagoya University, Chikusa-ku, Nagoya 464-8603, Japan

yashima@apchem.nagoya-u.ac.jp

Received October 20, 2009



A series of monomeric strands consisting of *m*-terphenyl backbones with chiral rigid *C*-linked (**3**) and flexible *N*-linked (**5**) formamidines and achiral carboxylic acid (**4**) and flexible carboxymethyl (**6**) residues were synthesized, and their duplex formations through amidinium–carboxylate salt bridges were investigated by NMR, circular dichroism (CD), and UV–visible spectroscopies. The salt bridge-derived duplex formation was largely dependent on the structures of the formamidine and carboxylic acid strands, and the *C*-linked formamidine strand **3** formed a more stable duplex with the complementary carboxylic acid strands (**4** and **6**) than did the flexible *N*-linked formamidine strand **5**. The single crystal X-ray analysis revealed that the duplex **5**·**4** has a skewed right-handed double helical structure. A complementary duplex dimer was also synthesized from the dimers of **5** and **4** joined by diacetylene linkers. Variable-temperature CD measurements indicated that the duplex possesses a dynamic double helical structure resulting from the flexible *N*-linked formamidine units.

Introduction

The double helix of DNA has attracted significant interest because of its key biological structure and functions, for example, the storage and faithful transmission of genetic

information from generation to generation. Consequently, chemists have devoted considerable efforts to the design and synthesis of artificial double helical oligomers and polymers not only to mimic the structure and functions of DNA, but also to develop advanced chiral materials.^{1–8} In contrast to a wide variety of synthetic oligomers and polymers folding into single-stranded helical conformations,⁹ only a few motifs are available for constructing double-helical structures.^{1–8} Most of these motifs, however, lack the key feature of DNA, that is, the complementarity of the strands.

*To whom correspondence should be addressed.

(1) For reviews on synthetic double helices, see: (a) Lehn, J.-M. *Supramolecular Chemistry: Concepts and Perspectives*; VCH: Weinheim, Germany, 1995. (b) Nielsen, P. E. *Acc. Chem. Res.* **1999**, *32*, 624–630. (c) Albrecht, M. *Chem. Rev.* **2001**, *101*, 3457–3498. (d) Huc, I. *Eur. J. Org. Chem.* **2004**, 17–29. (e) Albrecht, M. *Angew. Chem., Int. Ed.* **2005**, *44*, 6448–6451. (f) Furusho, Y.; Yashima, E. *Chem. Rec.* **2007**, *7*, 1–11. (g) Amemiya, R.; Yamaguchi, M. *Chem. Rec.* **2008**, *8*, 116–127.

(2) For examples of helicates, see: (a) Lehn, J. M.; Rigault, A.; Siegel, J.; Harrowfield, J.; Chevrier, B.; Moras, D. *Proc. Natl. Acad. Sci. U.S.A.* **1987**, *84*, 2565–2569. (b) Koert, U.; Harding, M. M.; Lehn, J. M. *Nature* **1990**, *346*, 339–342. (c) Woods, C. R.; Benaglia, M.; Cozzi, F.; Siegel, J. S. *Angew. Chem., Int. Ed. Engl.* **1996**, *35*, 1830–1833. (d) Orita, A.; Nakano, T.; An, D. L.; Tanikawa, K.; Wakamatsu, K.; Otera, J. *J. Am. Chem. Soc.* **2004**, *126*, 10389–10396. (e) Katagiri, H.; Miyagawa, T.; Furusho, Y.; Yashima, E. *Angew. Chem., Int. Ed.* **2006**, *45*, 1741–1744.

(3) For examples of aromatic oligoamides that fold into double helices, see: (a) Berl, V.; Huc, I.; Khoury, R. G.; Krische, M. J.; Lehn, J.-M. *Nature* **2000**, *407*, 720–723. (b) Dolain, C.; Zhan, C.; Leger, J.-M.; Daniels, L.; Huc, I. *J. Am. Chem. Soc.* **2005**, *127*, 2400–2401. (c) Zhan, C.; Leger, J.-M.; Huc, I. *Angew. Chem., Int. Ed.* **2006**, *45*, 4625–4628. (d) Haldar, D.; Jiang, H.; Leger, J.-M.; Huc, I. *Angew. Chem., Int. Ed.* **2006**, *45*, 5483–5486. (e) Gan, Q.; Bao, C.; Kauffmann, B.; Grelard, A.; Xiang, J.; Liu, S.; Huc, I.; Jiang, H. *Angew. Chem., Int. Ed.* **2008**, *47*, 1715–1718.

Inspired by the complementary double helical structure of DNA, we have recently designed and synthesized a complementary double helical oligomer **1·2** with a controlled helix-sense that consists of two crescent-shaped *m*-terphenyl strands containing optically active formamidine and achiral carboxyl groups (Figure 1).^{8a} The duplexation relies on the amidinium–carboxylate salt bridges which are unique in binding structures composed of double hydrogen bonds and the electrostatic interaction between the basic amidines and carboxylic acids.¹⁰ The complementary face-to-face association between each *m*-terphenyl strand through the amidinium–carboxylate salt bridges leads to the well-defined, intertwined duplex. Due to the high association constant

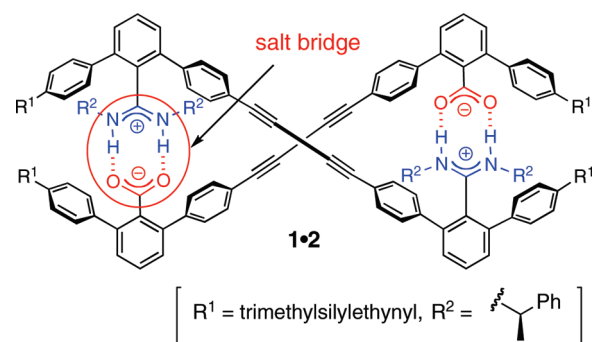


FIGURE 1. Artificial double helix **1·2** assisted by face-to-face salt bridge formation.

(4) For examples of anion-templated double helices, see: Sanchez-Quesada, J.; Seel, C.; Prados, P.; de Mendoza, J.; Dalcol, I.; Giralt, E. *J. Am. Chem. Soc.* **1996**, *118*, 277–278.

(5) For examples of helicene-based double helices, see: (a) Sugiura, H.; Nigorikawa, Y.; Saiki, Y.; Nakamura, K.; Yamaguchi, M. *J. Am. Chem. Soc.* **2004**, *126*, 14858–14864. (b) Sugiura, H.; Amemiya, R.; Yamaguchi, M. *Chem. Asian J.* **2008**, *3*, 244–260.

(6) For examples of oligoresorcinol-based double helices, see: (a) Goto, H.; Katagiri, H.; Furusho, Y.; Yashima, E. *J. Am. Chem. Soc.* **2006**, *128*, 7176–7178. (b) Goto, H.; Furusho, Y.; Yashima, E. *J. Am. Chem. Soc.* **2007**, *129*, 109–112. (c) Goto, H.; Furusho, Y.; Yashima, E. *J. Am. Chem. Soc.* **2007**, *129*, 9168–9174. (d) Goto, H.; Furusho, Y.; Miwa, K.; Yashima, E. *J. Am. Chem. Soc.* **2009**, *131*, 4710–4719. (e) Goto, H.; Furusho, Y.; Yashima, E. *Chem. Commun.* **2009**, 1650–1652.

(7) For examples of synthetic double helices based on phosphoric acid or pyridine–pyridone alternate co-oligomers, see: (a) Yamada, H.; Maeda, K.; Yashima, E. *Chem.—Eur. J.* **2009**, *15*, 6794–6798. (b) Abe, H.; Machiguchi, H.; Matsumoto, S.; Inouye, M. *J. Org. Chem.* **2008**, *73*, 4650–4661.

(8) For examples of double helices based on amidinium–carboxylate salt bridges, see: (a) Tanaka, Y.; Katagiri, H.; Furusho, Y.; Yashima, E. *Angew. Chem., Int. Ed.* **2005**, *44*, 3867–3870. (b) Furusho, Y.; Tanaka, Y.; Yashima, E. *Org. Lett.* **2006**, *8*, 2583–2586. (c) Ikeda, M.; Tanaka, Y.; Hasegawa, T.; Furusho, Y.; Yashima, E. *J. Am. Chem. Soc.* **2006**, *128*, 6806–6807. (d) Furusho, Y.; Tanaka, Y.; Maeda, T.; Ikeda, M.; Yashima, E. *Chem. Commun.* **2007**, 3174–3176. (e) Hasegawa, T.; Furusho, Y.; Katagiri, H.; Yashima, E. *Angew. Chem., Int. Ed.* **2007**, *46*, 5885–5888. (f) Maeda, T.; Furusho, Y.; Sakurai, S.-I.; Kumaki, J.; Okoshi, K.; Yashima, E. *J. Am. Chem. Soc.* **2008**, *130*, 7938–7945. (g) Ito, H.; Furusho, Y.; Hasegawa, T.; Yashima, E. *J. Am. Chem. Soc.* **2008**, *130*, 14008–14015.

(9) For reviews of synthetic oligomers and polymers with a single-stranded helical conformation, see: (a) Rowan, A. E.; Nolte, R. J. M. *Angew. Chem., Int. Ed.* **1998**, *37*, 63–68. (b) Gellman, S. H. *Acc. Chem. Res.* **1998**, *31*, 173–180. (c) Green, M. M.; Park, J.-W.; Sato, T.; Teramoto, A.; Lifson, S.; Selinger, R. L. B.; Selinger, J. V. *Angew. Chem., Int. Ed.* **1999**, *38*, 3138–3154. (d) Nakano, T.; Okamoto, Y. *Chem. Rev.* **2001**, *101*, 4013–4038. (e) Hill, D. J.; Mio, M. J.; Prince, R. B.; Hughes, T. S.; Moore, J. S. *Chem. Rev.* **2001**, *101*, 3893–4012. (f) Cornelissen, J. J. L. M.; Rowan, A. E.; Nolte, R. J. M.; Sommerdijk, N. A. J. M. *Chem. Rev.* **2001**, *101*, 4039–4070. (g) Brunsveld, L.; Folmer, B. J. B.; Meijer, E. W.; Sijbesma, R. P. *Chem. Rev.* **2001**, *101*, 4071–4098. (h) Fujiki, M. *J. Organomet. Chem.* **2003**, *685*, 15–34. (i) Yashima, E.; Maeda, K.; Nishimura, T. *Chem.—Eur. J.* **2004**, *10*, 42–51. (j) Maeda, K.; Yashima, E. *Top. Curr. Chem.* **2006**, *265*, 47–88. (k) *Foldamers: Structure, Properties, and Applications*; Hecht, S.; Huc, I., Eds.; WILEY-VCH: Weinheim, Germany, 2007. (l) Pijper, D.; Feringa, B. L. *Soft Matter* **2008**, *4*, 1349–1372. (m) Yashima, E.; Maeda, K. *Macromolecules* **2008**, *41*, 3–12. (n) Yashima, E.; Maeda, K.; Furusho, Y. *Acc. Chem. Res.* **2008**, *41*, 1166–1180. (o) Saraogi, I.; Hamilton, A. D. *Chem. Soc. Rev.* **2009**, *38*, 1726–1743.

(10) For examples of applications of amidinium–carboxylate salt bridges in supramolecular chemistry, see: (a) Terfort, A.; Kiedrowski, G. v. *Angew. Chem., Int. Ed. Engl.* **1992**, *31*, 654–656. (b) Kirby, J. P.; Roberts, J. A.; Nocera, D. G. *J. Am. Chem. Soc.* **1997**, *119*, 9230–9236. (c) Félix, O.; Hossaini, M. W.; De Cian, A.; Fischer, J. *Angew. Chem., Int. Ed. Engl.* **1997**, *36*, 102–104. (d) Wulff, G.; Schöenfeld, R. *Adv. Mater.* **1998**, *10*, 957–959. (e) Kraft, A.; Peters, L.; Powell, H. R. *Tetrahedron* **2002**, *58*, 3499–3505. (f) Corbellini, F.; Di Costanzo, L.; Crego-Calama, M.; Geremia, S.; Reinhoudt, D. N. J. *J. Am. Chem. Soc.* **2003**, *125*, 9946–9947. (g) Cooke, G.; Duclairoir, F. M. A.; Kraft, A.; Rosair, G.; Rotello, V. M. *Tetrahedron Lett.* **2004**, *45*, 557–560. (h) Rosenthal, J.; Hodgkiss, J. M.; Young, E. R.; Nocera, D. G. *J. Am. Chem. Soc.* **2006**, *128*, 10474–10483. (i) Sanchez, L.; Sierra, M.; Martin, N.; Myles, A. J.; Dale, T. J.; Rebek, J., Jr.; Seitz, W.; Guldi, D. M. *Angew. Chem., Int. Ed.* **2006**, *45*, 4637–4641. (j) Katagiri, H.; Tanaka, Y.; Furusho, Y.; Yashima, E. *Angew. Chem., Int. Ed.* **2007**, *46*, 2435–2439. (k) Otsuki, J.; Kanazawa, Y.; Kaito, A.; Islam, D. M. S.; Araki, Y.; Ito, O. *Chem.—Eur. J.* **2008**, *14*, 3776–3784.

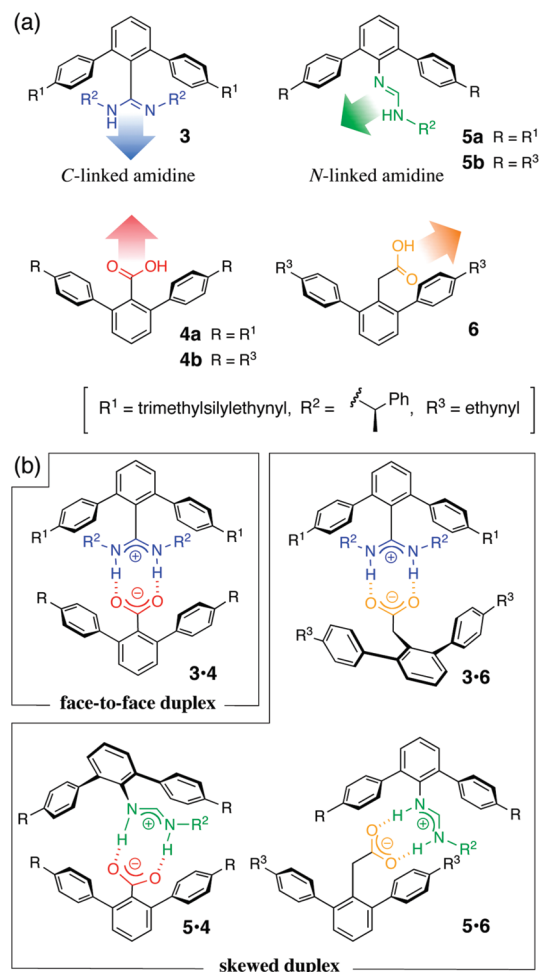
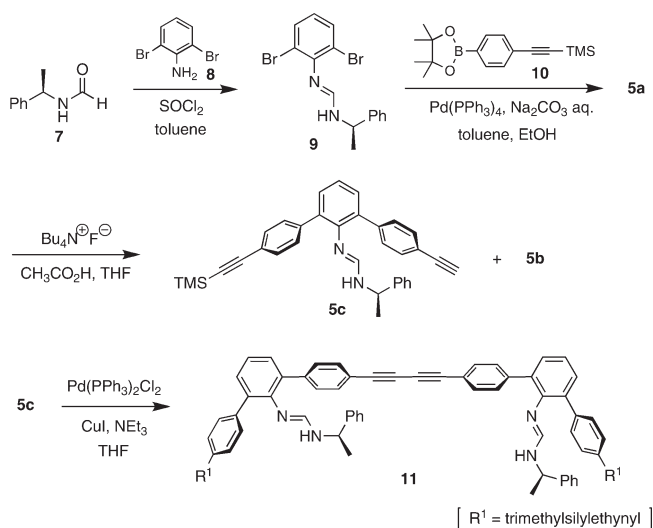


FIGURE 2. (a) Structures of chiral formamidines (**3** and **5**) and achiral carboxylic acids (**4** and **6**) and (b) schematic illustration of amidinium–carboxylate salt bridge formation.

and the rigid intertwined structure associated with the chiral formamidines, the resulting duplex has a thermodynamically stable one-handed double helical structure.^{8a,g} On the basis of this model oligomer study, the face-to-face salt bridge-assisted duplex (**3·4**) formation by the *C*-linked *m*-terphenyl formamidine **3** and the *m*-terphenyl formic acid **4** (Figure 2) has been used as a motif for creating various complementary double helical oligomers with different lengths and sequences,^{8b,d,e,g} and polymers^{8c,f} with a controlled

SCHEME 1. Synthesis of the Strands 5 and 11



handedness. We anticipated that the modification of the geometrical structure around the salt bridges would provide a novel complementary double helical motif. In this study, we designed and synthesized a series of novel skewed duplexes, such as **3·6**, **5·4**, and **5·6**, using chiral *N*-linked *m*-terphenyl formamidine **5** and/or achiral *m*-terphenyl acetic acid **6** in combination with the conventional strands **3** and **4** (Figure 2), and investigated their association behaviors and chiroptical properties. In addition, we also prepared a double helical dimer based on the skewed duplex motif **5·4** with the flexible *N*-linked formamidine units, and its preferred-handed helical structure in solution as compared to that of the dimer of **3·4** (**1·2** in Figure 1) was investigated by means of NMR, circular dichroism (CD), and UV–visible spectroscopies as well as the single crystal X-ray analysis of the model duplex **5·4**.

Results and Discussion

Synthesis of Monomeric and Dimeric Strands. The new chiral monomeric formamidine **5**, in which the *m*-terphenyl group is linked to one of the nitrogen atoms of the formamidine, and the corresponding dimer **11** joined by a diacetylene linker were prepared according to Scheme 1. The optically active formamide **7**, derived from (*R*)-1-phenylethylamine,¹¹ was allowed to react with dibromoaniline **8** and thionyl chloride, producing the formamidine **9** in 48% yield.¹² The Suzuki–Miyaura coupling of **9** with the boronate **10** afforded **5a**. Subsequently, **5a** was then treated with Bu₄N⁺F[−] to yield the monodesilylated formamidine **5c** (30%) along with the didesilylated formamidine **5b** (7% yield). **5c** was then dimerized by the oxidative coupling with use of Pd and Cu catalysts to give the dimeric strand **11** in 65% yield. The *m*-terphenyl acetic acid **6** was also prepared according to Scheme 2. The Suzuki–Miyaura coupling of the dichloride **12** with the boronic acid **13** catalyzed by Pd(OAc)₂ and the phosphine ligand **14**¹³ yielded the methyl

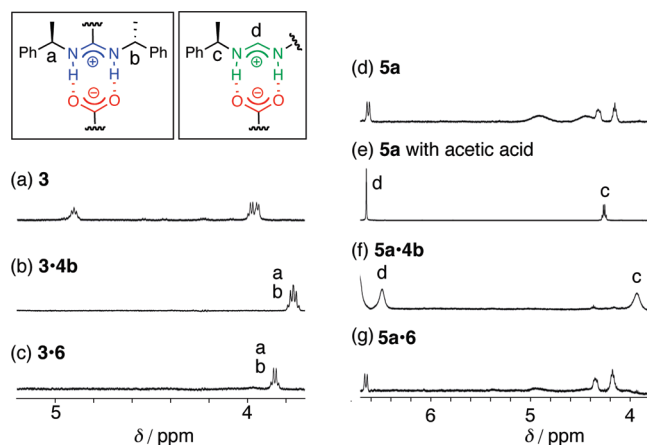
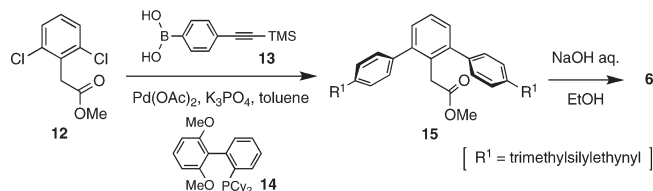


FIGURE 3. ¹H NMR (500 MHz, CDCl₃, rt) spectra of (a) **3** (4.9 mM), (b) **3·4b** (1 mM), (c) **3·6** (1 mM), (d) **5a** (117 mM), (e) **5a** (117 mM) with acetic acid (5 equiv), (f) **5a·4b** (1 mM), and (g) **5a·6** (1 mM).

SCHEME 2. Synthesis of the Strand 6



ester **15**, which was then hydrolyzed in an aqueous NaOH solution to give **6** in 95% yield. All the monomers and dimers were purified by column chromatography and characterized and identified with ¹H and ¹³C NMR spectroscopies, elemental analyses, and mass measurements (see the Experimental Section and the Supporting Information (SI)).

Duplex Formation of Monomeric Strands. We first investigated the duplex formation of the formamidines **3** or **5a** with the carboxylic acids **4b** or **6** in CDCl₃ by ¹H NMR spectroscopy. The formamidine **3** showed a complicated spectrum due to the presence of several conformers originating from the *E*–*Z* isomerism of the C=N double bonds and the restricted rotation about the C–C bond between the formamidine and *m*-terphenyl groups.^{8a} On the other hand, the ¹H NMR spectrum of **6** became simple, indicating the formation of the skewed duplex **3·6** in which the formamidine unit is most likely fixed in the *E* configuration through the salt bridge formation as in the case of the face-to-face duplex **3·4b** (Figure 3, and in the Supporting Information Figures S1 and S2).^{8a} The NH proton resonances of the **3·4b** appeared as a doublet peak at a low magnetic field of approximately δ 13.3 ppm (Supporting Information, Figure S1) due to the salt bridge formation, while the corresponding NH protons were not observed for **3·6** probably due to the fast monomeric strand–duplex equilibrium. The association constant of **3** and **6** estimated by ¹H NMR in CDCl₃ at 25 °C¹⁴ was 1.7 × 10⁵ M^{−1} (Supporting Information, Figure S6), which was lower than that of

(11) Iwata, M.; Kuzuhara, H. *Chem. Lett.* **1989**, *18*, 2029–2030.

(12) Gall, M.; McCall, J. M.; TenBrink, R. E.; VonVoigtlander, P. F.; Mohrland, J. S. *J. Med. Chem.* **1988**, *31*, 1816–1820.

(13) Walker, S. D.; Barder, T. E.; Martinelli, J. R.; Buchwald, S. L. *Angew. Chem., Int. Ed.* **2004**, *43*, 1871–1876.

(14) See the Supporting Information and: Connors, K. A. *Binding Constants: The Measurement of Complex Stability*; John Wiley & Sons: New York, 1987.

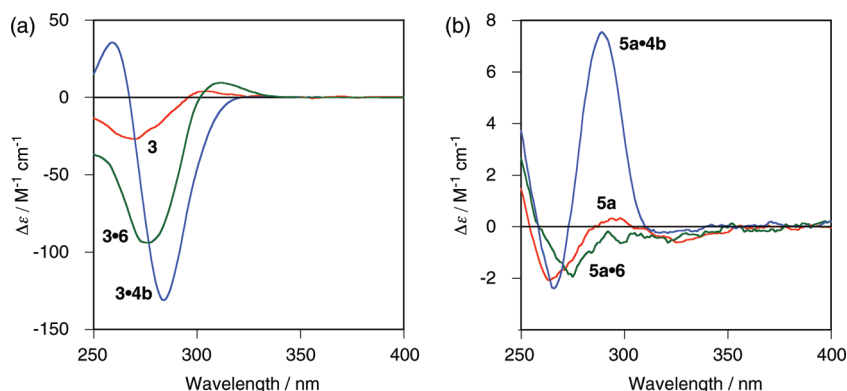


FIGURE 4. CD spectra of **3**, **3·4b**, **3·6** (a) and **5a**, **5a·4b**, and **5a·6** (b) at ca. 25 °C in CDCl₃ (1 mM).

3 and **4b** (ca. 10^6 M^{-1}),¹⁵ because of the relatively weaker acidity of the alkyl carboxylic acid **6** compared to that of the aryl carboxylic acid **4b**.¹⁶

The formamidine **5a** also showed a complicated ¹H NMR spectrum caused by a similar *E*–*Z* isomerism and tautomerism of the C=N double bonds (Figure 3d, and in the Supporting Information Figure S3). However, the spectrum showed clear signals after the addition of excess acetic acid, which can be ascribed to the formation of the amidinium–acetate salt bridges (Figure 3e). The ¹H NMR spectra of **5a** with **4b** also exhibited similar simple peaks, indicating the formation of the complementary skewed duplex **5a·4b** (Figure 3f, and in the Supporting Information Figure S3), although the broadening of the resonances and the lack of NH protons due to the salt bridge formation suggest a rather weak association of this system. In contrast, when **6** was used for the complexation with **5a** in CDCl₃, the observed spectrum of the mixture remained complicated, suggesting incomplete salt bridge formation (Figure 3g, and in the Supporting Information Figure S4). The association constants of **5a** with **4b** or **6** estimated by ¹H NMR in CDCl₃¹⁴ at 25 °C were 1.2×10^4 and $7.5 \times 10^2 \text{ M}^{-1}$, respectively (Supporting Information, Figure S6). The weaker basicity of **5a** relative to **3** is likely caused by the lack of the *N*-alkyl substituent on the formamidine group,¹⁷ resulting in the lower association constants for **5a·4b** and **5a·6** in comparison to those for **3·4b** and **3·6**, respectively.

The chiroptical properties of the chiral duplexes **3·4b**, **3·6**, **5a·4b**, and **5a·6** were then investigated by CD and absorption measured in CDCl₃ at ca. 25 °C (1 mM) (Figure 4, and in the Supporting Information Figure S5). The CD spectrum of **3·6** in CDCl₃, in which 93% of **3** and **6** are hybridized under the conditions based on the association constant, showed

clear CD signals below 330 nm, while **3** exhibited a weak Cotton effect in this region (Figure 4a). The CD intensity of the second Cotton effect ($\Delta\epsilon_{\text{second}}$) of **3·6** is about $-94 \text{ M}^{-1} \text{ cm}^{-1}$, which is approximately 3.5 times greater than that of **3** ($\Delta\epsilon_{\text{second}} = -27 \text{ M}^{-1} \text{ cm}^{-1}$). Although the CD intensity of **3·6** is relatively smaller than that of **3·4b** ($\Delta\epsilon_{\text{first}} = -131 \text{ M}^{-1} \text{ cm}^{-1}$), the remarkable enhancement of the Cotton effect upon the complexation of **3** with the achiral **6** and **4b** suggested the formation of a preferred-handed double helix consisting of intertwined complementary *m*-terphenyl units. In contrast, **5a** showed a very weak Cotton effect, because **5a** possesses a one chiral phenylethyl group and the stereogenic center is located relatively far from the *m*-terphenyl strand (Figure 4b). However, once complexed with the achiral **4b**, the CD spectral pattern significantly changed and its intensity drastically increased to form a duplex **5a·4b**, in which 75% of **5a** and **4b** are estimated to be complexed. These results suggest that the duplex likely adopts an excess one-handed double helical structure, although the CD intensity of the duplex was much weaker than that of the **3·4b**. On the other hand, no apparent Cotton effect enhancement was observed for **5a·6**, as expected from its low association constant in CDCl₃, indicating that **5a** and **6** may be too flexible to form a preferred-handed intertwined double helical structure.

The X-ray single-crystal analysis was then carried out to gain insight into the chiral structure of the skewed duplex **5·4**. The single crystals suitable for the X-ray structural analysis were obtained from a toluene/hexane solution of the skewed duplex **5b·4b** without the terminal trimethylsilyl groups. The crystal structure revealed that the duplex **5b·4b** adopts a right-handed double helical structure (Figures 5, and in the Supporting Information Figure S7 and Table S1). The formamidine and carboxy groups formed a salt bridge with two hydrogen bonds with an average N–O distance of 2.69 Å. Due to the *N*-linked formamidine residue, the two monomeric strands were held together in a skewed manner; the angle formed between two intersecting straight lines, passing through C¹⁰ and C¹³ of **5b** and C⁴¹ and C⁴⁴ of **4b**, is 123° (Figure 5c). The benzene rings of the formamidine-bound *m*-terphenyl group were chirally twisted clockwise by 49° and 53°, whereas those of the carboxy-bound *m*-terphenyl group were twisted counterclockwise by 56° and 61°. The preferential clockwise twists were observed for all the benzene rings of the *m*-terphenyl groups in the right-handed double helical **1·2**.^{8a} Therefore, the relatively weak Cotton

(15) Dilution ¹H NMR experiments were performed to estimate the association constants of **3** with **4b** and **11** with **16** in CDCl₃. These constants were observed that upon the dilution of the complexes **3·4b** (0.05 mM) and **11·16** (0.01 mM), no signals due to the dissociated amidine **3** and **11** could be detected (Supporting Information, Figures S1 and S8). On the basis of the results together with the detection limit, the association constants were roughly estimated. See ref 8a.

(16) The acidities of phenylacetic acid ($\text{p}K_{\text{a}} = 13.5$ and 11.6) in DMF and DMSO are relatively weaker than those of benzoic acid ($\text{p}K_{\text{a}} = 12.3$ and 10.9), respectively. See: Izutsu, K. *Acid-Base Dissociation Constants in Dipolar Aprotic Solvents*; IUPAC Chemical Data Series, No. 35; Blackwell Scientific: Oxford, UK, 1990.

(17) For examples of the substituent effects of amidines on basicity, see: (a) Raczynska, E.; Oszczapowicz, J. *Tetrahedron* **1985**, *41*, 5175–5179. (b) Oszczapowicz, J.; Ciszowski, K. *J. Chem. Soc., Perkin Trans. 2* **1987**, 663–668.

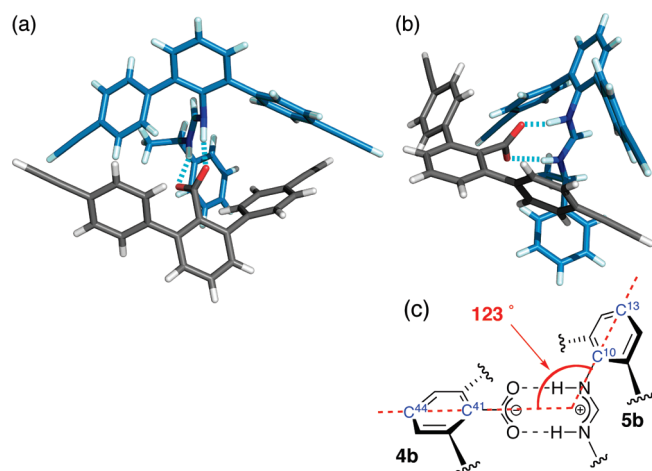


FIGURE 5. X-ray structure of **5b·4b**: (a) top view and (b) side view. Carbon, black or pale blue; oxygen, red; nitrogen, blue. The intermolecular hydrogen bonds between N and O with average N···O distances of 2.69 Å are shown by light blue dashed lines. (c) Schematic illustration of the geometry around the skewed salt bridge.

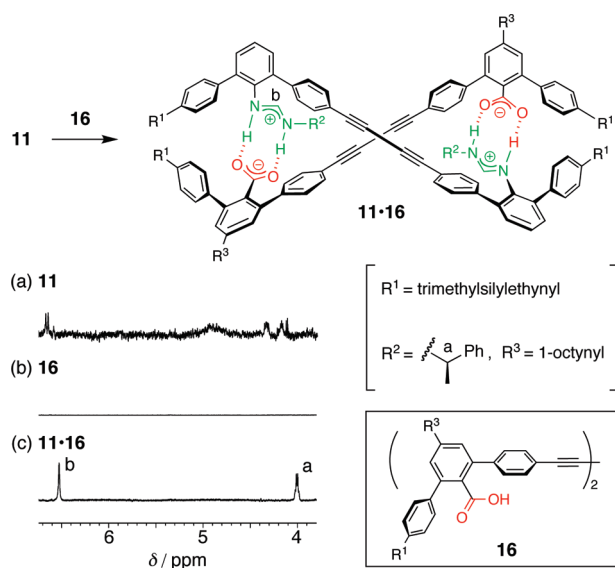


FIGURE 6. ^1H NMR (500 MHz, CDCl_3 , rt) spectra of (a) **11** (0.1 mM), (b) **16** (3.1 mM), and (c) **11·16** (0.1 mM).

effects observed in the **5a·4b** may be ascribed to the opposite twist-sense of the *m*-terphenyl groups.

Duplex Formation of Dimeric Strands of 5 and 4. On the basis of systematic studies on the complexation of complementary monomeric strands with different formamidine and carboxyl groups together with the crystal structural analysis of **5b·4b**, it was found that the newly designed flexible *N*-linked formamidine strand **5** could form a relatively stable intertwined duplex with the *m*-terphenyl formic acid strand **4**, therefore we then prepared dimers of **5** and **4** joined by diacetylene linkers **11** and **16**, respectively (Scheme 1), and its duplex formation was investigated. 1-Octynyl chains were introduced as a solubility enhancer in the dicarboxylic acid **16**.^{8g}

Due to the presence of a variety of conformational isomers, **11** showed a broad and quite complicated ^1H NMR spectrum in CDCl_3 (Figure 6a, and in the Supporting Information Figure S8). However, upon complexation with

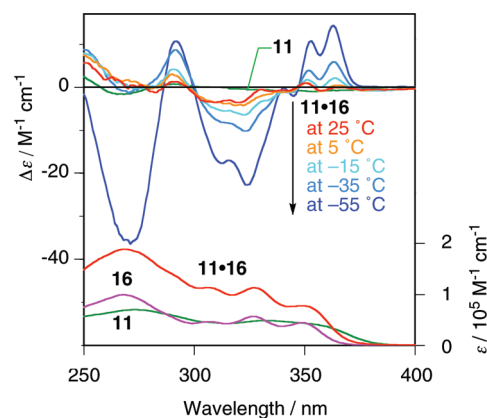


FIGURE 7. CD spectra of **11** (ca. 25 °C) and **11·16** (−55, −35, −15, 5, and 25 °C) and UV/vis spectra of **11**, **16**, and **11·16** (ca. 25 °C) in CDCl_3 . The concentrations of **11**, **16**, and **11·16** are 0.1, 0.1, and 0.02 mM, respectively.

16, the ^1H NMR spectrum became simple, indicating the duplex formation of the dimer **11·16**, although most of the signals remained broadened. The salt bridge formation was supported by the NH proton resonances that appeared as a broad peak at a lower magnetic field of δ 13.4 ppm. We noted that the corresponding NH proton resonances could not be observed for the monomer duplex **5a·4b**. Upon dilution of a solution of the duplex (0.01 mM), no signals due to the dissociated free **11** and **16** were observed. Thus, the dimeric skewed complex **11·16** formed a rather stable duplex stabilized by the double salt bridge formation. The association constant of **11** and **16** in CDCl_3 was roughly estimated to be greater than 10^6 M^{-1} .¹⁵

The duplex **11·16** showed weak, but apparent CD signals below 370 nm, whereas **11** exhibited very weak Cotton effects in this region (Figure 7). This remarkable enhancement of the Cotton effects for the duplex **11·16**, especially in the absorption region of the diacetylene linkages (ca. 300–370 nm), indicated that the duplex **11·16** most likely adopted a preferred-handed double helical structure, as in the case of the analogous duplex **1·2**.^{8a} In contrast to the thermodynamically stable, right-handed double helix (*R*)-**1·2**, the **11·16** showed significant changes in its CD intensity depending on temperature; the CD intensity in the diacetylene linkage region gradually increased with the decreasing temperature from 25 to −35 °C, and was drastically enhanced at −55 °C not only in the diacetylene linkage chromophore region, but also in the *m*-terphenyl absorption region (250–300 nm). These results clearly indicated that the duplex **11·16** has a dynamic nature and the diastereomeric right- and left-handed double helices are under equilibrium, which shifts to an excess of helices at low temperature. In addition, the dramatic increase in the Cotton effect intensity in the *m*-terphenyl absorption region suggests that the twist-sense of the *m*-terphenyl groups may also be significantly biased at −55 °C, although the twist-sense of the *m*-terphenyl groups of the monomeric duplex (**5b·4b**) was opposite to each other in the solid state (Figure 5). However, the observed CD intensity of **11·16** ($\Delta\epsilon_{\text{first}} = 14.4 \text{ M}^{-1} \text{ cm}^{-1}$ in CDCl_3 at −55 °C) is still much lower than that of the face-to-face complexed **1·2** ($\Delta\epsilon_{\text{first}} = -246 \text{ M}^{-1} \text{ cm}^{-1}$ in CDCl_3 at 20 °C).^{8a} Therefore, the helix-sense excess of **11·16** may be lower than that of **1·2**.

Summary

In summary, we have synthesized a series of monomeric and dimeric strands consisting of *m*-terphenyl backbones with rigid or flexible chiral formamidines and achiral carboxylic acid units. The duplex formation through the amidinium–carboxylate salt bridges is highly dependent on the structures of the formamidines and carboxylic acids, and the *C*-linked formamide strand appeared to form a more stable duplex with the complementary carboxylic acid strands than the *N*-linked formamide strand. The dimeric duplex **11**·**16** was found to possess a dynamic double helical structure probably caused by the flexible skewed *N*-linked formamide units. This finding may be useful to develop unique complementary double helical oligomers and polymers with dynamic characteristics.^{9c,d,h,j,m,n}

Experimental Section

Materials. Copper(I) iodide (CuI) and palladium acetate (Pd(OAc)₂) were obtained from Kishida (Osaka, Japan). Tetrakis(triphenylphosphine)palladium(0) (Pd(PPh₃)₄) and bis-(triphenylphosphine)palladium(II) dichloride (Pd(PPh₃)₂Cl₂) were purchased from Tokyo Kasei (TCI, Tokyo, Japan). (*R*)-*N*-(1-Phenylethyl)formamide (**7**),¹¹ 4-(trimethylsilylethynyl)-phenylboronic acid (**13**),¹⁸ carboxylic acids **4a**^{8a} and **4b**,^{8c} and dicarboxylic acid **16**^{8g} were synthesized according to the previously reported methods.

Synthesis of (*R*)-*N*-(2,6-Dibromophenyl)-*N'*-(1-phenylethyl)-formamide (9**).** SOCl₂ (121 mg, 1.02 mmol) was added dropwise to a solution of 2,6-dibromoaniline (**8**) (251 mg, 1.00 mmol) and **7** (172 mg, 1.16 mmol) in anhydrous toluene (1.00 mL). The resultant suspension was stirred at room temperature for 1 h and at 65 °C for 16 h. After nitrogen was bubbled through the solution for 1 h, the solvent was evaporated under reduced pressure. The residue was then purified by column chromatography (NH–SiO₂, hexane/CHCl₃ = 9/1 to 4/1) to afford **9** (186 mg, 48%) as a white solid. Mp: 84.7–86.8 °C. IR (KBr, cm⁻¹): 3247 (ν_{N–H}), 1644 (ν_{C=N}). ¹H NMR (300 MHz, CDCl₃, **9** (69 mM), CH₃CO₂H (5 equiv)): δ 7.49 (d, *J* = 8.0 Hz, 2H), 7.44–7.18 (m, 6H), 6.83 (t, *J* = 7.8 Hz, 1H), 4.61 (q, *J* = 6.9 Hz, 1H), 1.65 (d, *J* = 6.8 Hz, 3H). ¹³C NMR (126 MHz, CDCl₃, **9** (69 mM), CH₃CO₂H (5 equiv)): δ 158.5, 142.6, 142.5, 132.3, 128.9, 127.9, 127.1, 126.3, 120.3, 55.8, 23.3. Anal. Calcd for C₁₅H₁₄Br₂N₂: C, 47.15; H, 3.69; N, 7.33. Found: C, 46.96; H, 3.57; N, 7.18.

Synthesis of 5a. To a mixture of **10** (61.0 mg, 0.203 mmol), **9** (30.0 mg, 78.4 μmol), and Pd(PPh₃)₄ (9.06 mg, 7.84 μmol) were added EtOH (0.32 mL) and anhydrous toluene (0.79 mL) followed by an addition of aqueous Na₂CO₃ (2 M, 0.26 mL, 0.520 mmol). The mixture was refluxed for 17 h under stirring. After cooling, water (10 mL) was added to the reaction mixture and the mixture was extracted with Et₂O (2 × 10 mL). The organic extracts were washed with water (10 mL) and brine (10 mL) and then dried over anhydrous MgSO₄. After filtration, the solvent was removed by evaporation. The residue was then purified by column chromatography (NH–SiO₂, hexane/CHCl₃ = 10/0 to 4/1) to afford **5a** (13.9 mg, 31%) as a yellowish solid. Mp: 111.5–111.7 °C. [α]_D²⁰ +14.9 (*c* 0.39, CH₂Cl₂). IR (KBr, cm⁻¹): 3422 (ν_{N–H}), 2156 (ν_{C=C}), 1639 (ν_{C=N}). ¹H NMR (500 MHz, CDCl₃, **5a** (117 mM), CH₃CO₂H (5 equiv)): δ 7.51 (d, H₃, 5, 3', 5', *J* = 7.7 Hz, 4H), 7.38 (t, H₅, *J* = 6.7 Hz, 1H), 7.35–7.23 (m, H₄, 6', 4, 6, 4', 6', *m*- and *p*-H of Ph, 9H), 6.83 (d, *o*-H of Ph, *J* = 7.7 Hz, 2H), 6.63 (s, N=CH, 1H), 4.25–4.18 (m,

CHN, 1H), 1.37 (d, CH₃CHN, *J* = 6.3 Hz, 3H), 0.29 (s, TMS, 18H). ¹³C NMR (176 MHz, CDCl₃, **5a** (47 mM), CH₃CO₂H (5 equiv)): δ 156.9, 140.3, 138.7, 138.0, 133.7, 132.2, 130.4, 129.5, 129.0, 128.01, 127.96, 126.2, 122.6, 104.7, 95.3, 56.5, 21.9, 0.07. MS (FAB): *m/z* 569 [M + H]⁺. Anal. Calcd for C₃₇H₄₀N₂Si₂: C, 78.12; H, 7.09; N, 4.92. Found: C, 77.98; H, 6.86; N, 4.79.

Synthesis of 5c and 5b. A solution of Bu₄N⁺F⁻ in THF (0.100 mL, 1.68 mL, 0.168 mmol) was added portionwise (140 μL at a time) to a solution of **5a** (163 mg, 0.287 mmol) and acetic acid (36.7 mg, 0.611 mmol) in anhydrous THF (6.60 mL). After stirring for 10 min, aqueous HCl (1 M, 1.0 mL) and water (50 mL) were sequentially added. The mixture was then extracted with Et₂O (2 × 50 mL). The organic extracts were washed with water (50 mL) and brine (50 mL) and then dried over anhydrous MgSO₄. After filtration, the solvent was removed by evaporation. The residue was subjected to SEC fractionation to obtain **5c** (42.9 mg, 30%) as a yellowish solid and **5b** (8.8 mg, 7.2%) as a white solid.

5c: Mp: 57.8–58.0 °C. IR (film, cm⁻¹): 3418 (ν_{N–H}), 3294 (ν_{C=CH}), 2155 (ν_{C=C}), 1644 (ν_{C=N}). ¹H NMR (700 MHz, CDCl₃, **5c** (57 mM), CH₃CO₂H (5 equiv)): δ 7.54 (d, 2H, *J* = 8.1 Hz), 7.51 (d, *J* = 8.4 Hz, 2H), 7.40 (t, *J* = 7.6 Hz, 1H), 7.35–7.23 (m, 9H), 6.83 (d, *J* = 7.1 Hz, 2H), 6.63 (s, 1H), 4.23 (q, *J* = 6.8 Hz, 1H), 3.16 (s, 1H), 1.37 (d, *J* = 6.9 Hz, 3H), 0.29 (s, 9H). ¹³C NMR (176 MHz, CDCl₃, **5c** (57 mM), CH₃CO₂H (5 equiv)): δ 156.9, 140.0, 138.63, 138.57, 138.4, 137.9, 133.4, 132.4, 132.2, 130.5, 130.4, 129.6, 129.5, 129.1, 128.1, 128.0, 126.3, 122.6, 121.6, 104.7, 95.3, 83.3, 78.1, 56.5, 21.8, 0.08. HRMS (ESI+): *m/z* calcd for C₃₄H₃₃N₂Si (M + H⁺) 497.2413, found 497.2425.

5b: Mp: 175.7–175.9 °C. IR (KBr, cm⁻¹): 3435 (ν_{N–H}), 3292 (ν_{C=CH}), 2107 (ν_{C=C}), 1631 (ν_{C=N}). ¹H NMR (500 MHz, CDCl₃, **5b** (12.1 mM), CH₃CO₂H (10 equiv)): δ 7.54 (d, 4H, *J* = 7.9 Hz), 7.42–7.31 (m, 7H), 7.31–7.22 (m, 3H), 6.84 (m, 2H), 6.66 (s, 1H), 4.25–4.18 (m, 1H), 3.16 (s, 2H), 1.36 (d, *J* = 6.9 Hz, 3H). ¹³C NMR (176 MHz, CDCl₃, **5b** (15.8 mM), CH₃CO₂H (17 equiv)): δ 157.0, 140.2, 138.5, 138.4, 134.1, 132.4, 130.5, 129.7, 129.1, 128.1, 127.8, 126.3, 121.5, 83.3, 78.1, 56.4, 22.0. HRMS (ESI+): *m/z* calcd for C₃₁H₂₅N₂ (M + H⁺) 425.2018, found 425.2000.

Synthesis of 11. A mixture of **5c** (24.0 mg, 48.3 μmol), Pd(PPh₃)₂Cl₂ (3.3 mg, 4.7 μmol), CuI (1.0 mg, 5.4 μmol), and Et₃N (0.060 mL) in anhydrous THF (1.18 mL) was stirred at room temperature for 6 h. After evaporation to dryness, the residue was then purified by SEC chromatography (Biobeads SX-3, CHCl₃) to afford **11** (15.5 mg, 65%) as a yellow powder. Mp: 181 °C dec. [α]_D²⁰ +24.5 (*c* 0.29, CH₂Cl₂). IR (KBr, cm⁻¹): 3422 (ν_{N–H}), 2156 (ν_{C=C}), 1647 (ν_{C=N}). ¹H NMR (700 MHz, CDCl₃, **11** (14 mM), CH₃CO₂H (10 equiv)): δ 7.60 (d, *J* = 7.6 Hz, 4H), 7.52 (d, *J* = 7.6 Hz, 4H), 7.45–7.23 (m, 20H), 6.86 (d, *J* = 5.7 Hz, 4H), 6.65 (s, 2H), 4.22 (m, 2H), 1.38 (d, *J* = 6.7 Hz, 6H), 0.29 (s, 18H). ¹³C NMR (176 MHz, CDCl₃, **11** (14 mM), CH₃CO₂H (10 equiv)): δ 157.0, 140.3, 139.0, 138.6, 138.3, 138.1, 134.1, 132.8, 132.2, 130.6, 130.4, 129.9, 129.6, 129.1, 128.1, 127.8, 126.2, 122.6, 121.1, 104.7, 95.3, 81.6, 74.9, 56.5, 22.1, -0.1. Anal. Calcd for C₆₈H₆₂N₄Si₂: C, 82.38; H, 6.30; N, 5.65. Found: C, 82.16; H, 6.39; N, 5.53.

Synthesis of 15. A mixture of **12** (542 mg, 2.47 mmol), **13** (2.00 g, 9.18 mmol), Pd(OAc)₂ (13.0 mg, 57.5 μmol), K₃PO₄ (2.92 mg, 13.8 μmol), and **14** (52.1 mg, 0.123 mmol) in anhydrous toluene (9.50 mL) was stirred at 100 °C for 10 h. Water (50 mL) was added to the reaction mixture and the mixture was extracted with Et₂O (2 × 50 mL). The organic extracts were washed with water (50 mL) and brine (50 mL) and then dried over anhydrous MgSO₄. After filtration, the solvent was removed by evaporation. The residue was then purified by column chromatography (SiO₂, hexane/Et₂O = 10/0 to 99/1) to afford **15** (399 mg, 34%) as a white solid. Mp: 149.5–149.8 °C. IR (KBr, cm⁻¹): 2158

(18) Thoresen, L. H.; Jiao, G.-S.; Haaland, W. C.; Metzker, M. L.; Burgess, K. *Chem.—Eur. J.* **2003**, *9*, 4603–4610.

($\nu_{C=C}$), 1736 ($\nu_{C=O}$). $^1\text{H NMR}$ (500 MHz, CDCl_3): δ 7.49 (d, $J = 8.5$ Hz, 4H), 7.36 (t, $J = 7.2$ Hz, 1H), 7.25 (d, $J = 8.4$ Hz, 4H), 7.23 (d, $J = 7.6$ Hz, 2H), 3.45 (s, 3H), 3.42 (s, 2H), 0.26 (s, 18H). $^{13}\text{C NMR}$ (126 MHz, CDCl_3): δ 172.4, 142.9, 141.7, 131.8, 129.7, 129.3, 129.0, 127.0, 122.1, 104.8, 94.7, 51.8, 36.6, 0.0. HRMS (ESI+): m/z calcd for $\text{C}_{31}\text{H}_{34}\text{NaO}_2\text{Si}_2$ ($\text{M} + \text{Na}^+$) 517.1995, found 517.2002.

Synthesis of 6. A mixture of **15** (30.3 mg, 62.9 μmol) and aqueous NaOH (2.5 M, 0.78 mL) in EtOH (2.00 mL) was stirred at room temperature for 5 days. After an addition of water (10 mL), the mixture was washed with Et_2O (10 mL) and the aqueous layer was acidified with aqueous HCl (1 M). The precipitated solid was extracted with Et_2O (2×10 mL) and the organic extracts were dried over anhydrous MgSO_4 . After filtration, the solvent was removed by evaporation. The residue was then purified by SEC chromatography (Biobeads SX-3, CHCl_3) to afford **6** (20.1 mg, 95%) as a white powder. Mp: 202.3 °C dec. IR (KBr, cm^{-1}): 3195 ($\nu_{\text{O-H}}$), 2103 ($\nu_{C=C}$), 1715 ($\nu_{C=O}$). $^1\text{H NMR}$ (500 MHz, CDCl_3 , **6** (40 mM)): δ 7.54 (d, $J = 8.4$ Hz, 4H),

7.39 (t, $J = 7.4$ Hz, 1H), 7.28 (d, $J = 8.5$ Hz, 4H), 7.25 (d, $J = 6.1$ Hz, 2H), 3.50 (s, 2H), 3.13 (s, 1H). $^{13}\text{C NMR}$ (126 MHz, CDCl_3 , **6** (40 mM)): δ 176.9, 142.8, 141.8, 132.1, 129.4, 129.1, 128.9, 127.2, 121.3, 83.3, 77.8, 36.3. Anal. Calcd for $\text{C}_{24}\text{H}_{16}\text{O}_2$: C, 85.69; H, 4.79. Found: C, 85.39; H, 4.86.

Acknowledgment. This work was supported in part by a Grant-in-Aid for Scientific Research (S) from the Japan Society for the Promotion of Science (JSPS) and the Global COE Program "Elucidation and Design of Materials and Molecular Functions" of the Ministry of Education, Culture, Sports, Science, and Technology, Japan.

Supporting Information Available: Experimental procedures and characterization data for the monomeric duplexes **3·4b**, **3·6**, **5a·4b**, and **5a·6**, and the dimeric duplex **11·16**. This material is available free of charge via the Internet at <http://pubs.acs.org>.